Chapter 3

Hydrogen Gas Detection by Mini-Raman Lidar

Tatsuo Shiina

Additional information is available at the end of the chapter

http://dx.doi.org/10.5772/intechopen.74630

Abstract

Now, Hydrogen gas is of particular interest as new energy source and dangerous material in nuclear facility. Fuel cell is started to use in home power generation system in 2008 and fuel cell vehicle (FCV) is commercialized from 2014 in Japan. On contrary, the Great East Japan Earthquake revealed the fear of hydrogen explosion on Fukushima Nuclear Power plant in 2011. Contact type hydrogen sensors induce changes on the gas flow, and the actual concentration cannot be known. It is hard to get the gas concentration distribution in hydrogen leakage area. We focused on optical remote sensing for the hydrogen detection. Raman scattering detection was accomplished for the hydrogen gas with a compact Diode Pumped Solid State (DPSS) laser-based Raman lidar. The quantitative measurement was conducted on the hydrogen gas concentration of 1 - 100% and the detectable distance of <50 m. Next, a LED-based mini Raman lidar was developed with the same optical design as the former one in viewpoints of its robust operation and usability in the nuclear facility. The high-speed photon counter was developed to follow the high repetition frequency of LED pulse of >500 kHz, and the quantitative measurements of hydrogen concentration were conducted on lab-experiment and at outdoor.

Keywords: hydrogen, lidar, Raman, scattering, LED

1. Introduction

Nowadays, there is a strong demand for remote sensing in near range. Needless to say, the fear of terrorism, the human daily lives whether at urban or at countryside have the threat of non-safety. The urban polluted air, smoke on chemical factory, dust from construction site pose a threat to human social activities. Certain dangerous gas detections in volcanic zone, construction site, and water inspection, air quality check in factory, hall, park, and so on, are desired for safe life. Certain gas/dust monitoring in construction site, and air quality estimation in daily

life circumference are included in such demands for the improvement of working condition in factory and facility.

In the viewpoint of safety management, the working condition focus on the dust and leaked gas detections under construction site at outdoor. The mass media concerns to the atmospheric suspended materials represented as SPM (Suspended Particle Material), PM10/PM2.5, yellow sand, pollens, and also industrial dusts as dioxin, photochemical smog, and asbestos. The dust flow information, including the nuclear material, is strongly desired after the Great East Japan Earthquake. On indoor application, chemical gas flow in a factory, dust density measurement and dangerous gas monitoring such as CO, CO_2, CH_4, and H_2S in a tunnel construction site in mountain and under the sea are essential for such safety managements.

At the atmospheric monitoring indoor and outdoor, the "contact" sensors are utilized. These sensors are compact, cheap, and easy-to-use, while they need a lot to cover the whole area. A lot of sensors should be scattered in a certain area to get the target distribution and behavior. Low concentration gas and shooting out gas is difficult to perform the quantitative measurement [1, 2].

The word "LIDAR (Light Detection And Ranging)" is sometimes written as LiDAR for hard target detection and lidar for soft target detection. The former is utilized as a range finder to detect the distance up to the target. The latter is for monitoring the target condition and behavior at a certain distance. It is an ideal technique to monitor the suspended materials such as aerosol, dust, gas, and atmosphere remotely and safely [3–5]. Unlike a transmissometer which consists of an separated pair of transmitter and receiver, lidar can fix at a point and scan the observing direction. Then it can cover a certain area remotely. Lidar can obtain the distribution and change of the target in monitoring site by scanning the observation direction. Its observation range is enough long of a few to a hundred kilometers. In contrary, recently it applied for near range monitoring within a few hundred meters. Its application is industrial use.

Lidar technique utilizes various kinds of scattering. Mie scattering, Rayleigh scattering, Raman scattering, and so on. Mie scattering is generated by larger materials such as aerosols and dusts, while the Rayleigh scattering is caused by smaller materials such as molecules configuring the atmosphere. Raman scattering is brought about every material but it shifts wavelength of scattering light from the incident light one. It is convenient for target gas detection.

In this study, we developed the compact Raman lidar for hydrogen gas detection. To prevent the explosion accident of hydrogen gas, the sensor should detect the target gas of the low concentration of 1/4 of the explosion limit. In the case of hydrogen gas, its concentration is 1% [6–8]. The optical intensity of the lidar transmitter is designed to be safe for human eye and skin. This study has been started to apply for leaked gas detection in a hydrogen gas station [9, 10]. After that it has expanded to adapt to the nuclear facility. This lidar should be compact and easy-to-use. It is also applied to monitor the air qualities of working environment including hydrogen gas, atmospheric nitrogen gas and water vapor.

This report states the developments of the Diode Pumped Solid State (DPSS) laser-based compact Raman lidar and the LED-based mini-Raman lidar. At first Raman scattering and lidar principle are briefly mentioned, and after that, the development of concrete Raman lidars

is explained. Some results of quantitative measurements are shown with actual observation data.

2. Hydrogen generation – controlled and unprepared

Utilization of hydrogen energy is undergoing, which is led mainly by the Agency for Natural Resources and Energy in the Ministry of Economy, Trade and Industry, Japan to promote the spread of fuel cell car (FCV) and home-use fuel cell system.

Fuel cell generates electricity by chemical reaction between hydrogen and oxygen. It causes only water vapor and its power generation efficiency exceeds 30%. Hydrogen gas is stored in a high-pressure tank at 35 MPa in hydrogen station and FCV. 96 hydrogen stations were built in 2016 in Japan, and it will increase 160 stations in 2020. FCV were installed 2000 cars in 2016, and bus and forklift truck types were installed into on-site, too. The agency aims to expand it up to 40,000 cars in 2020. Now, FCV seems to conceal itself under electric vehicle (EV). FCV, however, can drive for a long travel distance of 700–850 km at one-time insufflations of hydrogen of 3 min [11]. For that reason, EV is good for small automobile for short distance, while FCV has a merit for large-size automobile for long distance.

Home-use fuel cell system is established its technologies in complex with cogeneration. Hydrogen is generated from urban gas or LP gas, and chemically reacts with oxygen, then generates the electricity. Exhaust heat on electricity generation is utilized to the other purpose (for example hot water supply). 200,000 systems have been already installed up to 2016. Reducing the price of the system is undergoing.

Hydrogen gas on the nuclear reactor is generated by the different process against the above. In general, the nuclear fuel rod boils water with its high temperature in nuclear reaction. At the Great East Japan Earthquake, it is considered that the tragic event was caused by the following process. The nuclear reactor was stopped automatically, while the fuel cell rod continued heating. Because the cooling system was fallen down, the water level was lowered and the rod was naked. Although the nuclear fuel rod was covered with zirconium, it reacted with water on the high temperature. As a result, zirconium took oxygen away from the water, the hydrogen gas was generated.

Under the controlled condition to generate the electricity or the unforeseen circumstances, hydrogen gas monitoring is essential and should prevent the accident.

3. Optical sensing for hydrogen gas

Hydrogen is flammable gas. It explodes at the concentration of >4% under the oxygen circumference [12]. The Fire Defense Agency defined that the gas sensor must have the minimal detection of the one fourth of the explosion limit of the target gas. It is essential to detect such flammable gas before the risk of its explosion. Methane, Carbon oxide, and so on have

absorption lines in the near infrared spectrum, and the differential absorption technique can be adapted for these gas detections. The hydrogen gas, however, has its absorption line in < l10 nm and does not have any clear absorption lines in ultra violet, visible – near infrared spectra [13]. The hydrogen gas detection is only conducted by contact chemical sensors such as combustible material, catalyst materials (Pt or Pd), and semiconductor type (SnO_2) [1, 2]. These sensors are high-sensitive to detect its concentration of a few tens ppm, while it is hard to get the gas distribution in whole of monitoring site. Furthermore, the contact sensor disturbs the gas flow, and its sensing direction influences to the measurement value. Its response time is slow, too.

Hydrogen gas has strong Raman effect, which depends on material. Raman scattering shifts the wavelength of the scattering light from that of the incident light. In general, the intensity of Raman scattering is 3 digits smaller than that of the Mie scattering [14, 15]. When electrons in atmospheric molecules (or certain gas, atom, and so on) are resonant with photons, most photons are elastically scattered (it is Rayleigh scattering), such that the scattered photons have the same optical frequency and wavelength as the incident light (photons). A small fraction of such photons is scattered with a frequency different from the original frequency of the incident photons. The frequency shift is usually lower than and partially higher than the original; Stokes scattering as longer wavelength and anti-Stokes scattering as shorter wavelength. The interaction of light with a material in a linear region allows absorption and emission of a photon precisely matching the difference in energy levels of the interacting electron. The energy absorption of the molecules causes Stokes scattering, while the energy loss of the molecules generates the anti-Stokes scattering. Stokes scattering shifts the wavelength of the incident light to the longer side. Anti-Stokes scattering shifts that to the shorter side as shown in **Figure 1**. Intensity of Anti-Stokes scattering is smaller than that of Stokes scattering. In general, this trend is remarkably strong when the Raman shift becomes large. In this study, Stokes scattering of hydrogen gas is selected for the lidar detection target under these backgrounds.

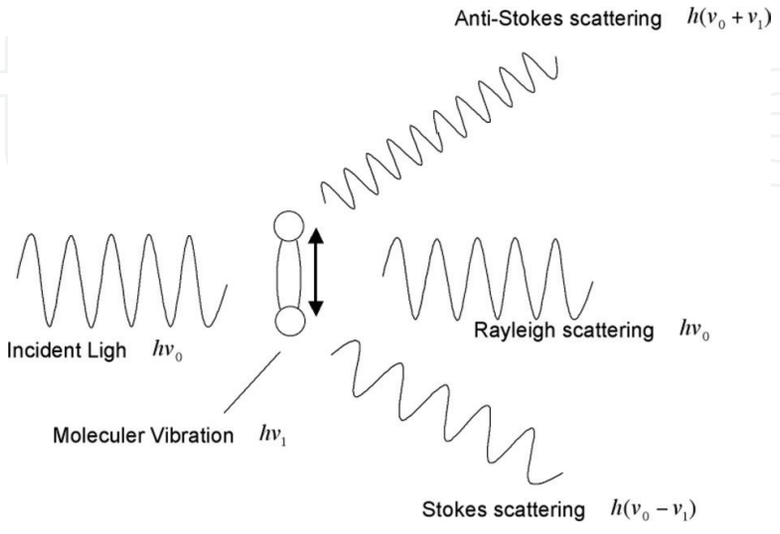

Figure 1. Raman scattering.

Target	Raman shift (cm^{-1})	Wavelength (nm)
Nitrogen	2331	380
Water vapor	3652	400
Oxygen	1556	369
Hydrogen	4160	408

Table 1. Raman shift and its wavelength against 349 nm light source.

To estimate the quantitative concentration of hydrogen gas, Raman scattering intensities of atmospheric nitrogen is utilized. When the concentration of hydrogen gas is negligible amount than that of atmospheric nitrogen, the ratio between the Raman scattering intensities of hydrogen gas and atmospheric nitrogen can indicate the concentration of the hydrogen gas quantitatively. The ratio is calibrated by the relative Raman scattering cross sections of hydrogen and nitrogen, which is about 3:1 [5]. **Table 1** shows the concrete Raman shifts and their shifted wavelengths against the 349 nm laser light source.

4. Compact Raman lidar

The principle of lidar is illustrated in **Figure 2**. The pulsed laser beam was collimated and fired into the atmosphere with almost parallel to the receiver's optical axis. The optical receiver is adjusted its field of view (FOV) to detect the lidar echo from the target with an adequate signal-to-noise ratio. The receiver's FOV decides the detecting range and the blind area, which the transmitting beam cannot enter within a receiver's FOV, especially in near range. It also affects the detecting intensity of the background light. As a traditional lidar has individual optics (biaxial optics) for a laser transmitter and a receiver, the system has a blind area. The blind area also causes in the case of coaxial optics that the beam is transmitted within a receiver's area. As FOV is wider, or the beam divergence is wider, the blind area will be shortened, while the background light enters a lot into the receiver. As a result, the signal-to-noise ratio of the lidar echo will be worse.

The lidar echo is detected by high sensitive detectors such as photomultiplier and Avalanche Photo Diode (APD), and stored in PC via digitizer. When the lidar echo becomes weak and hard to detect an analogue signal, photon counting method is selectable.

The compact lidar is suitable to the near range observation of less than a few hundred meters, while the traditional large lidar is good at the long-range observation from a few kilometers to a hundred kilometers. The compact lidar, however, is not a down-size one of the large lidar. **Table 2** shows the spatial and time scales in atmospheric phenomena. The large phenomena such as HP/LP have a large spatial and time scales, while the small phenomena like tornado takes small spatial and time scales. That is, the small phenomenon becomes small structure and quick motion. To detect and visualize such small phenomena, the compact lidar should follow to its quick motion with high resolution. Furthermore, near range detection is often a sensing in human living space. In that meaning, the transmitting optical power should be

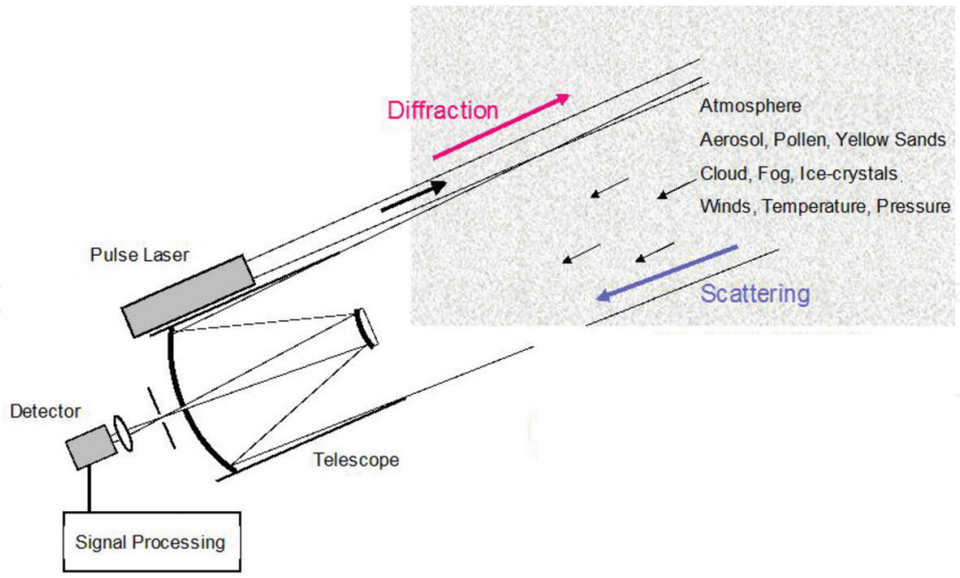

Figure 2. Lidar principle.

lower for eye-safety. It causes the limit of transmitting power and the selection of optical wavelength.

The Raman scattering intensity is estimated by Eq. (1).

$$P_R = \frac{\lambda_0}{\lambda_R} P_0 \chi \rho \sigma_R L \eta_D \tag{1}$$

where P_0, P_R are wavelength λ_0, λ_R of laser light source and Raman scattering intensity, respectively. χ is molar function of the target, ρ is number density of the molecules, σ_R is Raman scattering cross-section, L is pulse length and η_D is receiver's optical efficiency. The quantitative

Phenomena	Spatial scale	Time scale
HP/LP	1000 km	10 h
Typhoon	100 km	3 h
Convection	50 km	2 h
Thunder clouds	10 km	1 h
Cumulus	2 km	10 min
Down burst	600 m	7 min
Tornado	200 m	5 min
Boundary layer	60 m	10 s

Table 2. Spatial and time scales of atmosphere.

measurement is calculated by the intensity ratio of nitrogen echo and hydrogen echo. The lidar echo is inversely proportional to the distance to the power of square. But the above intensity ratio cancels the intensity decrease [6].

The concept of the hydrogen remote sensing is to install the "remote sensor" into the area monitoring in a hydrogen station. The sensor is put on a small car and monitors the inside area of the station on the street. In that meaning, the remote sensor should be compact. The eye-safety should be considered, too.

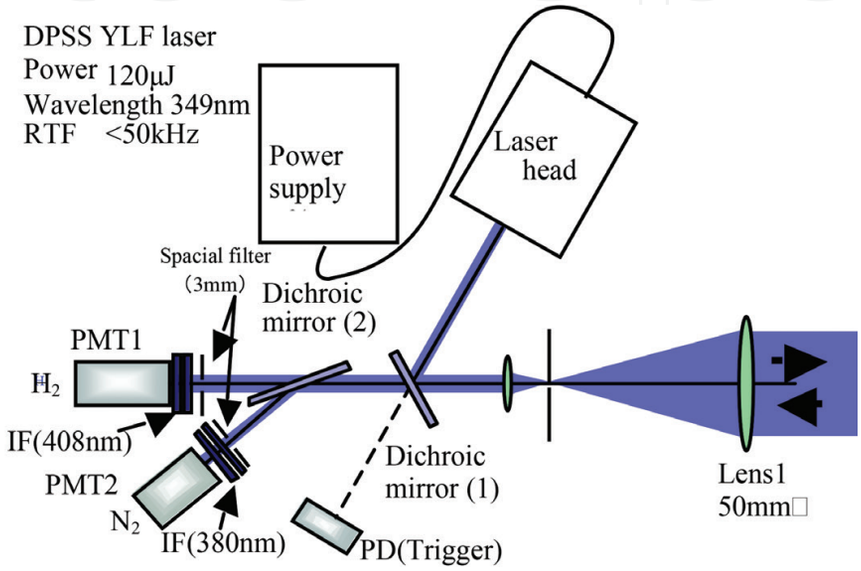

(a)

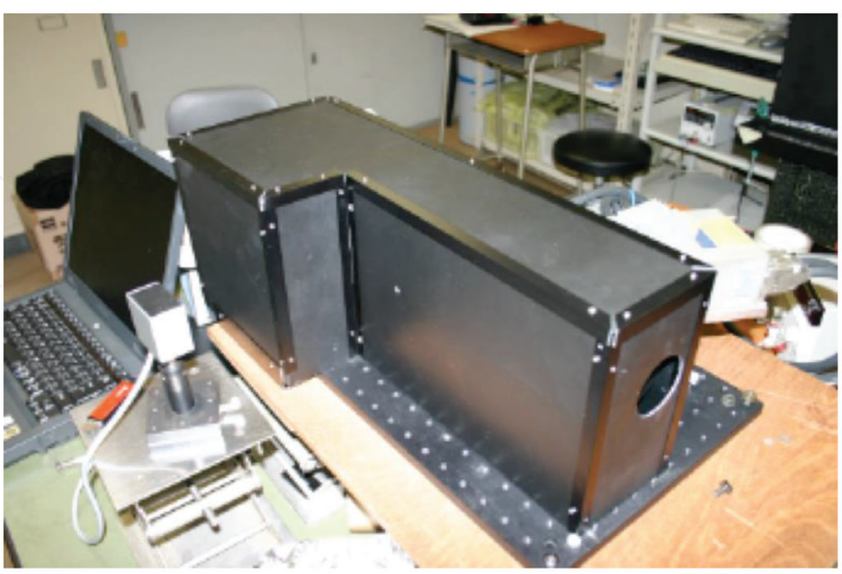

(b)

Figure 3. Optics of compact Raman lidar. (a) Compact Raman lidar—optical setup. (b) Outlook of compact Raman lidar.

In this study, we have developed the "in-line" type compact Raman lidar [16–21]. The in-line type optics has no blind area in principle. The in-line lidar has common optics for a transmitter and a receiver. An optical divider, here dichroic mirror, to separate the receiving echo and transmitting beam is installed. We designed and developed the compact Raman lidar to detect leaked hydrogen gas as minimum setup. It means that the system should be compact, light-weight and low electric power consumption. Our goal is the detection of the hydrogen gas concentration of 1% within the observation range of 0–50 m. The lidar optics is illustrated in **Figure 3**. The DPSS laser is utilized for lidar transmitting beam. Its power is 120 μJ and the wavelength is 349 nm. The receiver's aperture is 50 mmφ. The transmitting beam is expanded to 10 mmφ to be safe for human eye even in front of the system. The wavelength of the incident beam is decided to obtain the strong Raman signal. Shorter wavelength causes the larger Raman signal than the longer wavelength. The receiver's FOV was 2 mrad. The Raman shifted echoes passes through the first dichroic mirror (1), which is a divider, and echoes never returns to the light source. The Raman echoes are divided by the second dichroic mirror (2) depending on the wavelength for each Raman detection. The detectors are PMTs; one is for hydrogen gas (408 nm) and the other is for atmospheric nitrogen gas (380 nm). The interference filters of the wavelength widths of 3 nm are fixed on their PMTs. The nitrogen signal is used to estimate the quantitative concentration of hydrogen gas. The system size is 58 × 36 × 23 cm. It can put on the small desk.

Figure 4 shows the detected Raman echo of atmospheric nitrogen. Its signal was obtained from 1.5 to 50 m. The nearest echo in 0–1.5 m in **Figure 4(a)** was spoiled because of the misalignment and the aberration of the lenses. **Figure 4(b)** shows the range-corrected nitrogen Raman echo, which is corrected by the square of the distance and the overlap function between the transmitter and the receiver. The corrected echo intensity becomes flat and the fluctuation is minimum at any point within the observation range. The constant intensity indicates stable concentration of atmospheric nitrogen. This nitrogen echo is utilized to estimate the concentration of hydrogen gas in the observation range by taking the ratio between them.

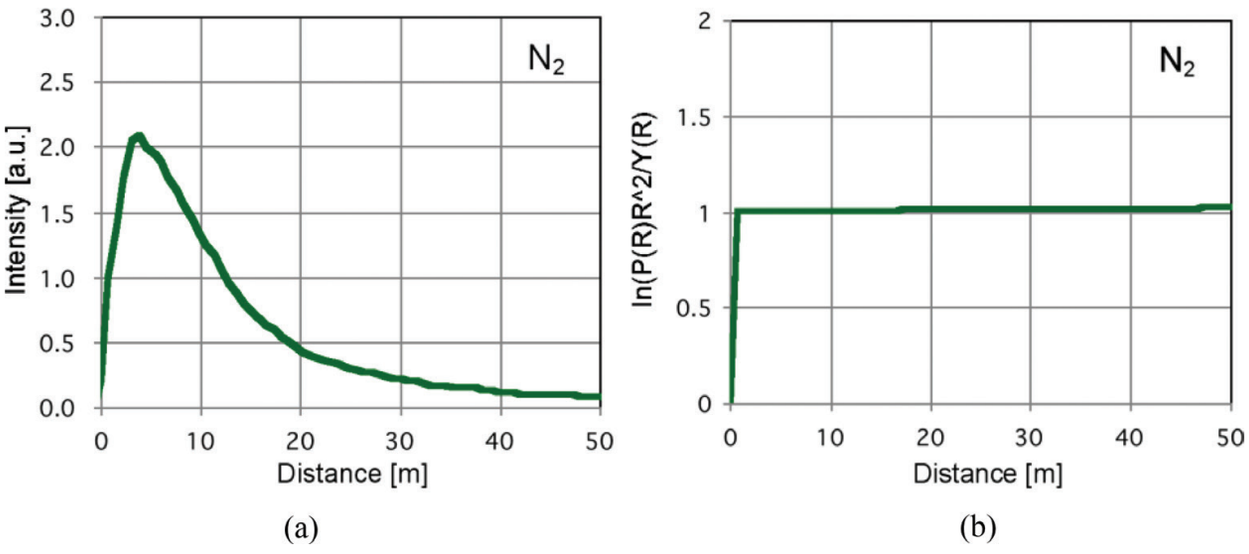

Figure 4. Lidar echo of atmospheric nitrogen gas. (a) A-scope signal. (b) Range-corrected data.

A quantitative measurement of the Raman scattering echo intensity from hydrogen gas was conducted. The hydrogen gas was filled in a gas cell of the size of 10 cm cube, of which window is quartz. The cell was positioned at a distance of 7–8 m from the lidar system and put with a small tilt against the optical axis to reduce the reflection and fluorescent lights to return the lidar. Although the reflection and fluorescence lights appear on the hydrogen and nitrogen echoes, they can be subtracted out. Furthermore, the Raman echo from hydrogen gas fluctuates in actual gas leaks, and it can be separated from the reflection and fluorescence lights from a hard target, which are constant in time. The observation distance of 8 m is defined as the safe distance for the explosion protection of hydrogen gas. The lidar echo was measured by an oscilloscope with a photomultiplier tube (PMT) operating in analogue mode.

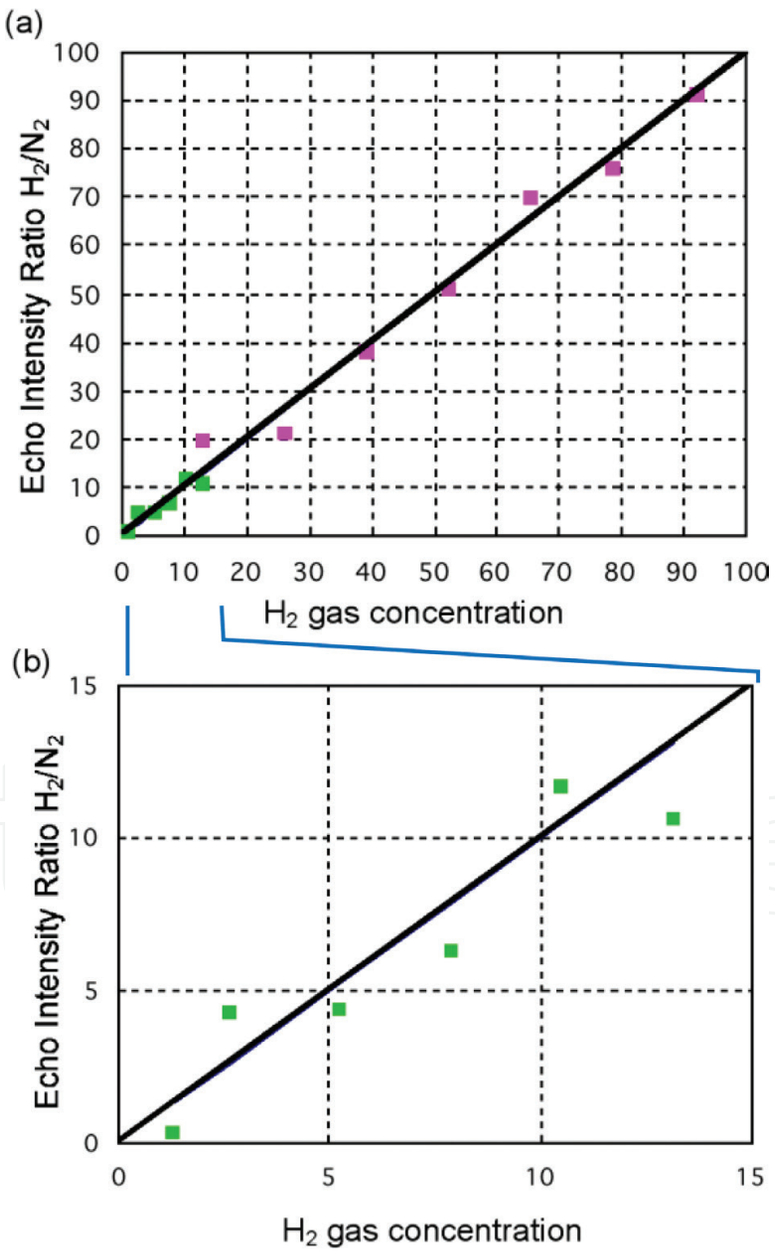

Figure 5. Estimation of hydrogen gas concentration. (a) High concentration of about 10–100% and (b) low concentration of 0–15%.

The echo intensity was obtained by the developed Raman lidar system. The concentration of hydrogen gas was controlled by adjusting the gas pressure in the cell. The results are shown in **Figure 5**, for (a) high concentration of about 10–100% and (b) enlarge graph of low concentration of 0–15%. These results were calibrated by subtracting the reference signal of the empty gas cell. The summation was about 30,000 shots. It is equal to a measurement time of about 30 s. The echo intensity ratio is linearly proportional to the hydrogen gas concentration. The result indicates the successful estimation down to the low concentration of 1%. The estimation error becomes less than ±1%. The fluctuation in the echo intensity was mainly due to the background light, unstable power of the laser beam and thermal noise of the detector. The actual leaked gas fluctuates more drastically.

5. LED-based mini-Raman lidar

The developed DPSS-based compact Raman lidar is designed to be eye-safe, while it is hard to install it into a certain monitoring site. The laser beam is possible to focus on a point, and it is not acceptable especially in dangerous gas environment because of its ignition. It is also hard to use it at outdoor with no AC power supply. In such demands, we started to develop the LED-based mini-Raman lidar with low optical power.

At first, we had the experiment to obtain the minimum power to detect the Raman echo of hydrogen gas as shown in **Figure 6**. The laser beam is entered into the quartz-windows cell filled with hydrogen gas. The hydrogen gas concentration was 100%. The Raman scattering echo was detected at the vertical direction. It is because the Raman intensity becomes maximum at the perpendicular direction against the optical axis of the transmitting beam. The

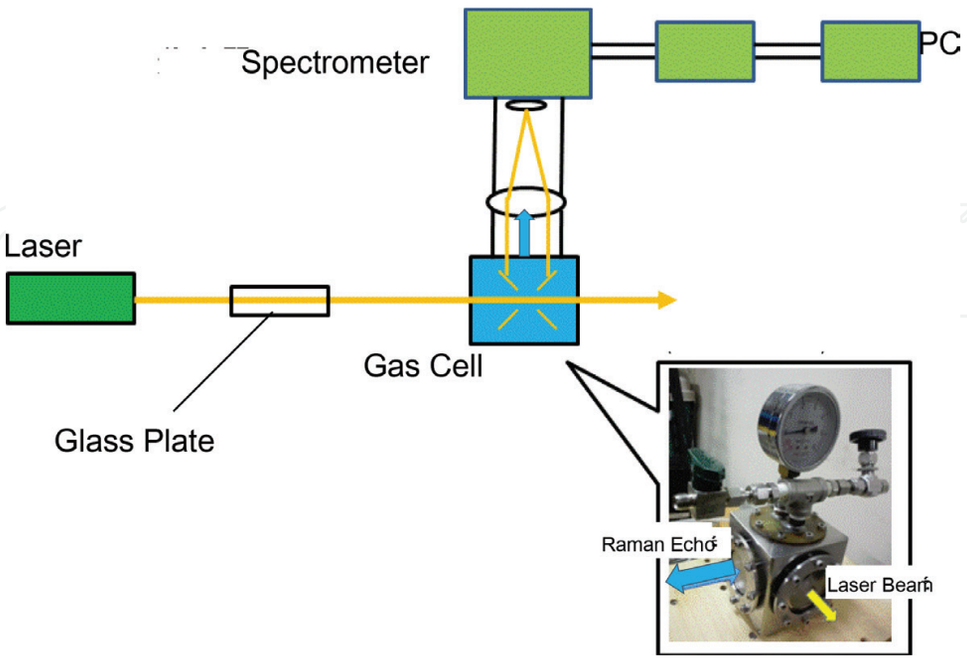

Figure 6. Verification of Raman scattering echo measurement with the minimum light intensity.

laser power was gradually decreased up to the Raman detection limit, which is estimated 1 W (=10 nJ/10 ns) by the numerical analysis. The reflection light by the glass plate was utilized to decrease the laser intensity efficiently and stably. The experimental result is shown in **Figure 7**. It shows that the Raman scattering echo was successfully detected by the estimated optical power of the transmitting beam.

Considering the above results, we developed the LED-based mini-Raman lidar. The lidar optics is biaxial type and the gas detection method is as same as the laser based compact Raman lidar as shown in **Figure 3**. The LED lamp module of the optical power of 1 W was used as the lidar light source. The wavelength of LED light is 365 nm, and the wavelengths of Raman scattering echoes become 400 nm for atmospheric nitrogen, 420 nm for water vapor and 430 nm for hydrogen gas with the same Raman shift shown in **Table 1**. The LED mini-Raman lidar optics is shown with photo in **Figure 8**. The optical setup is the same as the DPSS-laser based compact Raman lidar. The LED-based Raman lidar added the water vapor port by changing the optical interference filter with a filter wheel. All of the wavelength widths of the interference filters were 10 nm. It is the same width the used LED spectrum.

Although LED beam is hard to collimate, it never focuses after the transmission. It gives advantage in the closed space in the viewpoint of human safety concern. In this study, the transmitting beam was enlarged to 50 mmφ. Its divergence was about 10 mrad. The LED pulsed power was <1 W (=10 nJ/10 ns), while the pulse repetition frequency was 500 kHz. The receiving telescope was Cassegrain type of the aperture of 127 mmφ. The receiver's FOV was 3 mrad. The transmitting power is so weak, and the echo detection is photon counting with photomultipliers.

The system is so compact and handy that one can use it in any observation direction. The system power consumption is about 2 W and can operate with a small PC battery in 8–10 h. The observation range is aimed up to 20–30 m for hydrogen Raman signal. This observation range design comes from the facility space of a nuclear reactor to detect the hydrogen gas leakage. The specifications are summarized in **Table 3**.

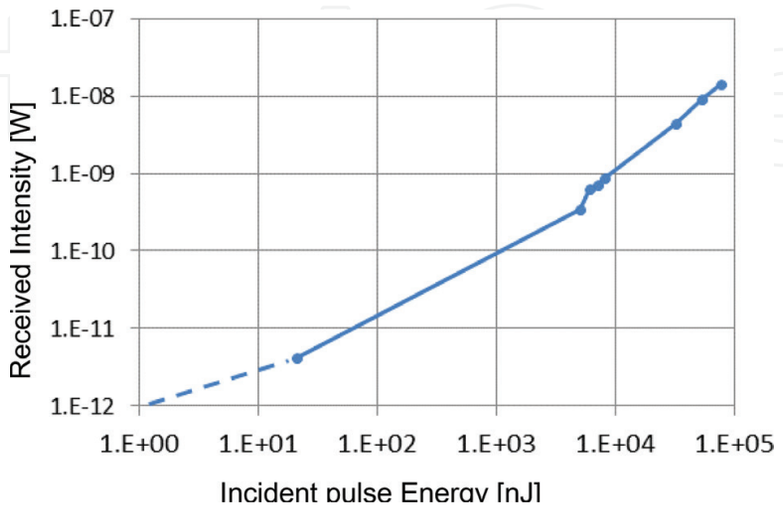

Figure 7. Raman scattering echo detection with lowered incident power.

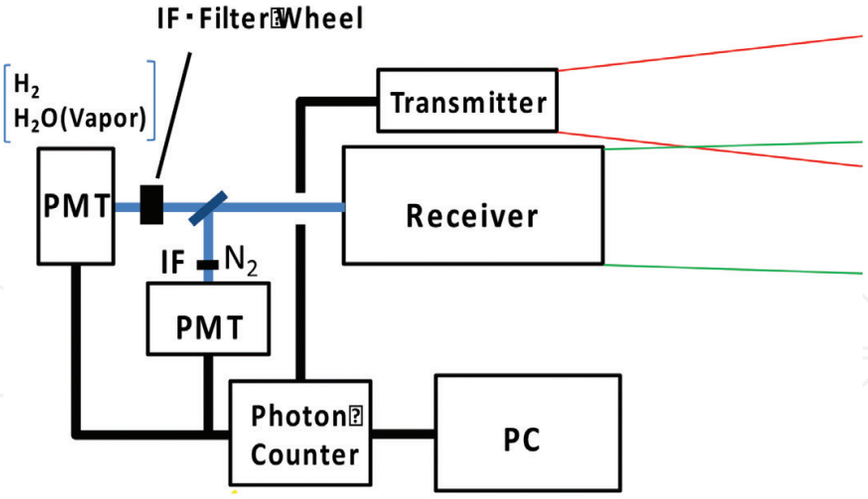

(a)

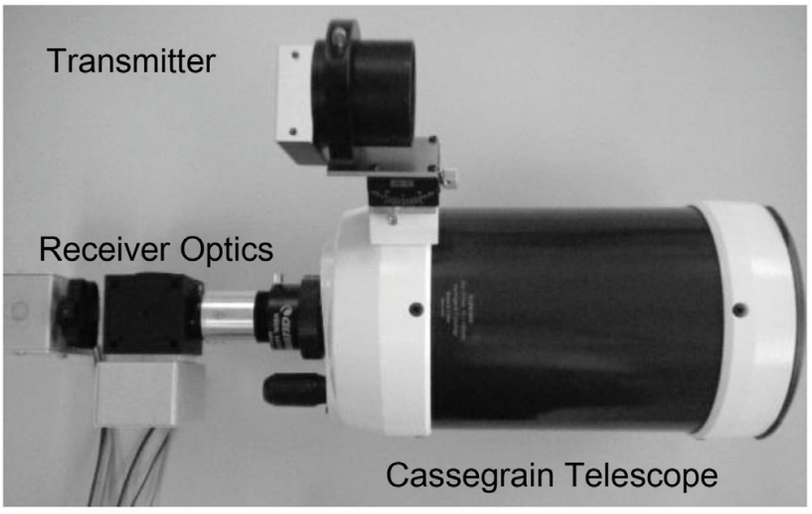

(b)

Figure 8. LED mini-Raman lidar. (a) Optical structure. (b) Lidar setup.

The high-speed photon counter was developed, too. It can follow the pulse repetition frequency of >500 kHz. Its time resolution is 1 ns. It is equivalent to the spatial (distance) resolution of 0.15 m. It has 2 channels, and their simultaneous measurements are possible with a single input or output trigger signal.

Figure 9 shows the observed Raman echo of the atmospheric nitrogen gas and the water vapor. The observation direction is nearly horizontal. The experiment was conducted in night time. Trees were captured at 80 m ahead. Accumulation was 3.5 min. Nitrogen echo was

Transmitter	
LED Pulse Power	750mW
Wavelength	365nm
Beam Diameter	50mmϕ
Beam Divergence	10mrad.
Repetition Frequency	>450kHz
Receiver	
Telescoe	Cassegrain
Diameter	127mmϕ
Field of View	<5mrad.
Interferene Filter	$\Delta\ \lambda$ =10nm
Detector	Photomultiplier

Table 3. Specifications of LED mini-Raman lidar.

obtained up to 70 m (**Figure 9(a)**). After that the fluorescence echo of the tree was also detected at 80 m. The atmospheric nitrogen is stable and its echo waveform becomes smooth. On the other hand, the water vapor echo had fluctuation because of low counts (**Figure 9(b)**). It was drastically changed by depending on the humidity. In the figure, the humidity was 25% on Feb. 7 in fine day, while it was 90% on Feb. 9 in rain day. The observation range of the water vapor was 70 m, which is equal to that of the nitrogen echo. The fluorescence echoes of trees were detected, too.

The quantitative measurement of hydrogen gas was conducted with a large gas chamber as shown in **Figure 10**. The hydrogen gas chamber has an aperture of 200 mm and a length of 500 mm. Pyrex glass of 10 mm thickness was used for light path windows to restrict the fluorescent light. It was set 5 m ahead from the LED mini-Raman lidar. The transmitting beam was adjusted its optical path against the receiver's field of view to cross both of optical paths at the chamber.

The hydrogen gas concentration was adjusted by vacuuming the air inside the chamber of 0.5 Pa and inserting the 100% hydrogen. This procedure repeated twice, and the hydrogen gas concentration of 75% was prepared. We also confirmed the air and hydrogen gases were well mixed in the chamber. After the first measurement, hydrogen gas concentration set to half, that is, 37.5% by vacuuming the inside gas of 0.5 Pa and inserting the air. Repeating these procedures, hydrogen gas concentration was adjusted as 18.8%, 9.4%, 4.7%, and 2.4%.

Experimental results are shown in **Figure 11**. The accumulation time was 3.5 min. The hydrogen Raman echo was appeared on the fluorescent light from the Pyrex glass. **Figure 11** shows enlargement of the peak change of the echo signals. Depending on the hydrogen gas concentration, the peak counts were changed. The echo counts of hydrogen gas Raman signal were subtracted from the reference echo (0% hydrogen gas). The results were summarized in **Figure 12**. In **Figure 12(a)**, hydrogen Raman echo counts at each detected distance were

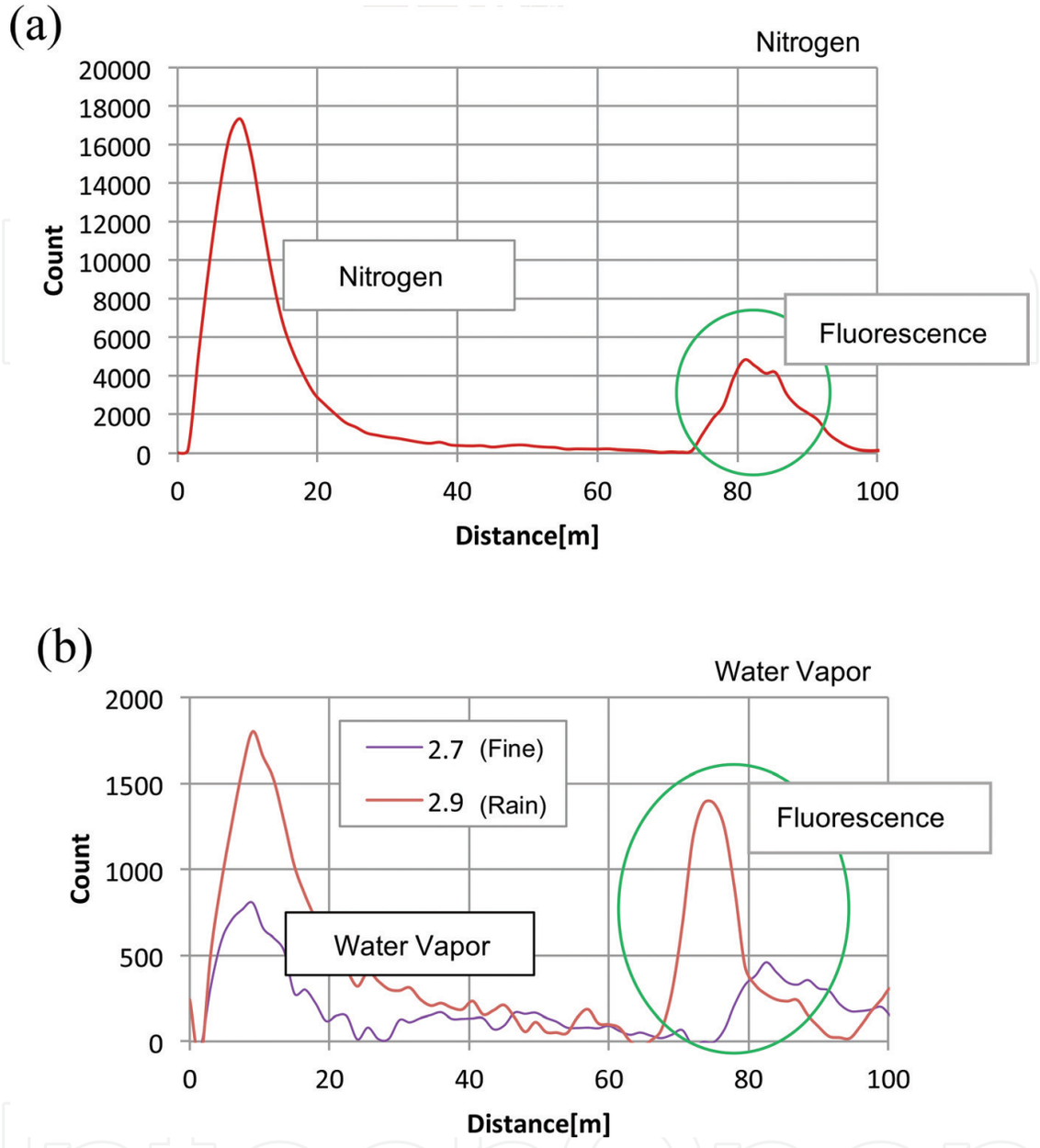

Figure 9. Atmospheric measurement by LED mini-Raman lidar. (a) Nitrogen Raman echo (b) Water Vapor echo.

graphed. The Raman echo counts at 5.25 and 5.4 m had the higher slant, while the firster (initial distance arising echo) and the later parts (main part of fluorescent light) of the peak signals showed lower slant. It means that the Raman scattering appears firster than the fluorescent light. The lidar counts at each distance in **Figure 12(a)** was summed as shown in **Figure 12(b)**. The errors were large, which came from the inexact concentration control of the hydrogen gas and the fluctuation of the fluorescent light, while the linear change was obtained down to the lowest concentration of a few percent. The Raman echo counts were remained at the 0% hydrogen gas concentration. We regarded hydrogen concentration after the procedure of vacuuming the content gas of 0.5 Pa and inserting the air two times as equal to 0%. It caused the remained echo counts at 0% concentration. And the fluctuation of the fluorescent light peak echo will cause it, too.

http://dx.doi.org/10.5772/intechopen.74630

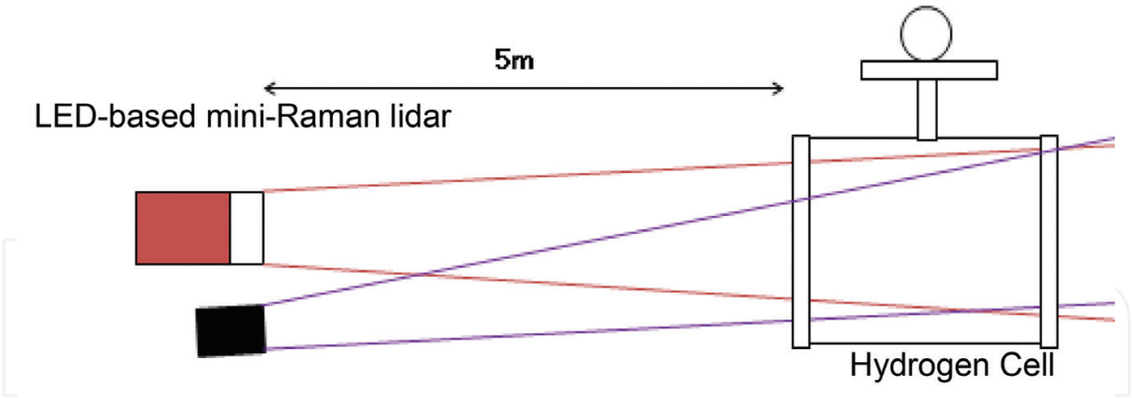

(a)

(b)

Figure 10. Hydrogen gas quantitative measurement. (a) Quantitative measurement of hydrogen gas. (b) System setup and arrangement.

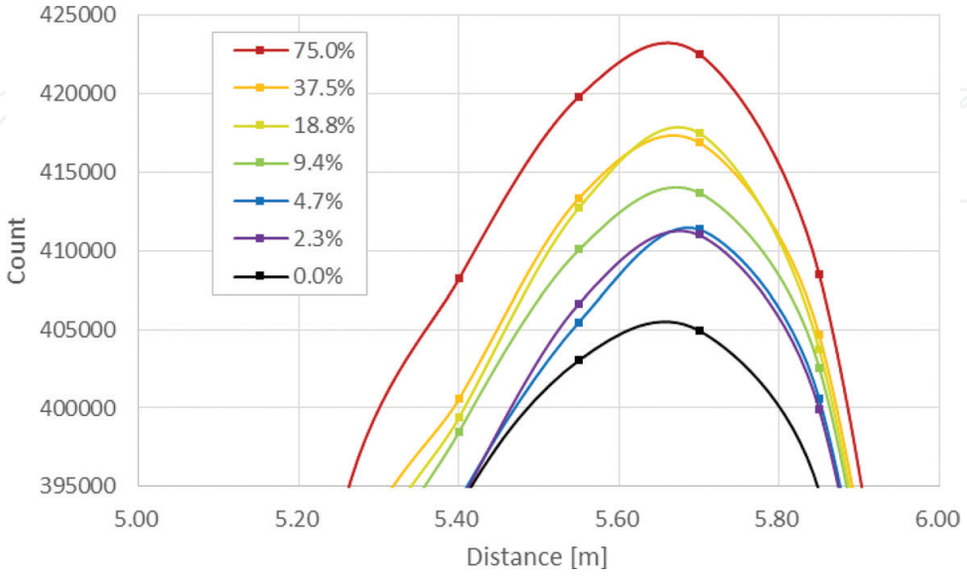

Figure 11. Peak signal changes depending on hydrogen gas concentration.

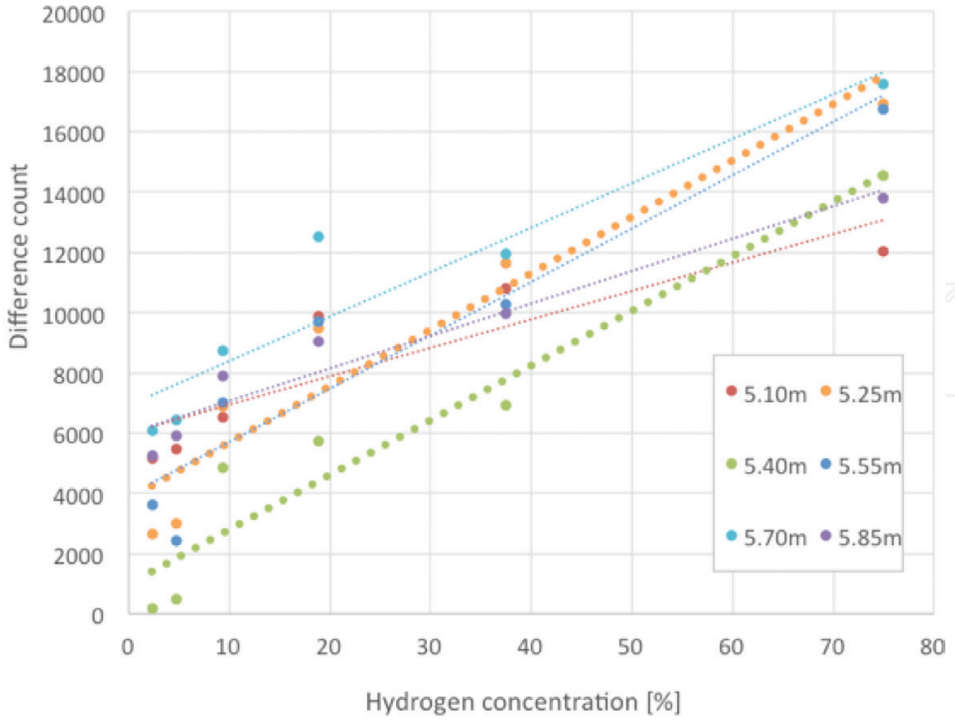

(a)

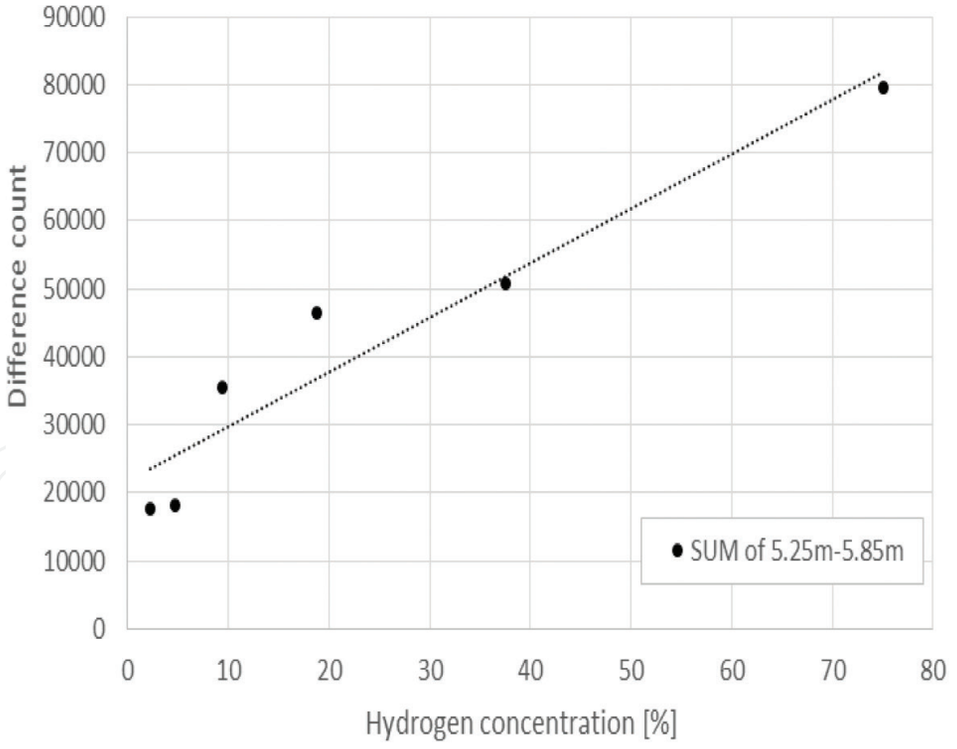

(b)

Figure 12. Change of hydrogen Raman echo counts depending on hydrogen gas concentration. (a) Echo changes at each detected distance. (b) Count sum at each concentration.

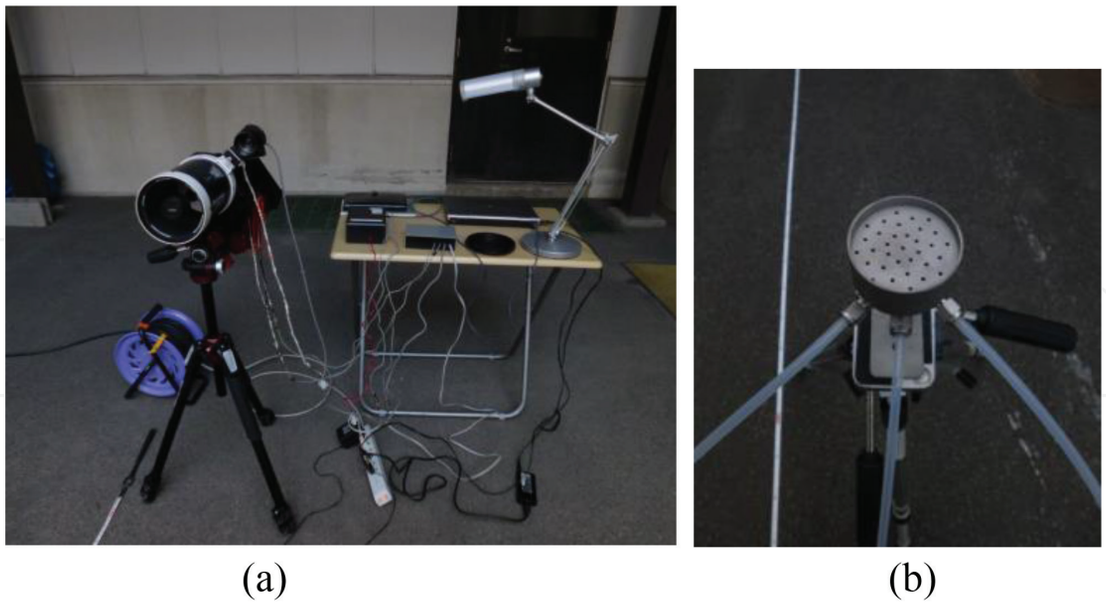

Figure 13. Hydrogen leakage measurement experiment outside. (a) LED mini-Raman lidar setup. (b) Hydrogen nozzle.

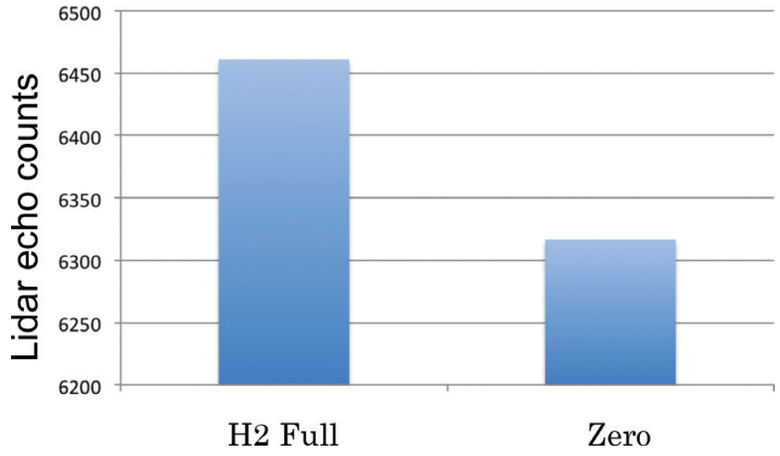

Figure 14. Measurement result of hydrogen leakage gas outside.

The hydrogen leakage experiment was conducted at outdoor in night time as shown in **Figure 13**. The hydrogen leakage nozzle shown in **Figure 13(b)** was fixed at 2.5 m ahead from the mini-lidar. The optical alignment between the transmitter and the receiver was adjusted to overlap fully. The leaked hydrogen gas was 50 l/min. The result is summarized in **Figure 14**. The accumulation time was 3.5 min. It is the result of 3 average times. The obvious difference between the hydrogen gas leakage and leakage stop conditions was obtained. The detected counts on the leakage stop condition were caused by the fluorescent light from the materials near the hydrogen nozzle. As compared with the lab experiment in **Figure 12**, the hydrogen Raman counts was low. The leakage gas volume, especially gas flow width against the optical axis was shorter than the hydrogen gas chamber or the optical pulse length. As a result, the

counts rate outdoor was smaller than the lab-experiment. After that, the authors repeated the quantitative measurement with more large chamber at the outdoor field. The same result in the lab-experiment was obtained.

6. Discussions

In the lab-experiment, that is, the hydrogen cell/chamber used experiments at indoor, the linear change of the lidar counts was obtained depending on the hydrogen concentration up to 1%. The accuracy is enough to evaluate the concentration quantitatively. The DPSS laser-based lidar can perform it within a few seconds by adequate setup. The LED-based lidar needs more time to evaluate the concentration. The evaluation error is remained on the current setup. At outdoor experiment, the obvious hydrogen Raman echo by the LED Raman lidar was detected at the gas leakage situation, while it is not easy to verify the concrete concentration. It is not only the system task, but also the gas flow fluctuation. As the leakage area was narrower than the pulsed beam length, the counts rate became lower. The accumulation time, beam size, and transmitting power intensity should be balanced to satisfy the demands.

The hydrogen gas detection is not only to estimate the precise concentration, but also on the easy-to-use and easy-to-install at on-site. The LED-based mini-Raman lidar is designed under this consideration. Its gas detection optics is as same as the laser-based Raman lidar, while the LED module is installed into the system. The observation range becomes short, while the system becomes so small, light-weight, low power consumption, and safe. The power consumption is enough small to operate with a small buttery. The LED-based mini-Raman lidar needs the accumulation time, and it is adequate to install it to the regular observation fixed on a certain position and monitor the stored gas on a ceiling. When Ultra Violet/Near Ultra Violet Laser Diode (UV/NUV-LD) is possible to utilize, the beam collimation will be improved and it can increase signal-to-noise ratio with the same optical pulse power. It will shorten the accumulation time, and become one of the solutions to detect the leakage hydrogen gas in the emergency case under no electrical power.

7. Conclusions

We developed the compact and the mini-Raman lidars for quantitative measurement of hydrogen gas. The current minimal detection limit of hydrogen gas concentration is 1% at the observation range of 0–50 m with DPSS-based compact lidar and 0–20 m with LED-based mini-lidar. The accumulation time is 30 s for the DPSS laser-based compact Raman lidar and 3.5 min for the LED-based mini-Raman lidar.

Now, the DPSS laser-based compact Raman lidar was improved to detect the ionization effect by nuclear materials. On contrary, the LED-based mini-Raman lidar expanded the target to the environmental measurement. The Raman scattering signal is a proof of a target gas existence. Each gas has its own Raman shift, and the optical sensing method of Raman lidar becomes one of solutions in the actual atmosphere, which contains complex materials.

The Raman signal is weak. It is 1/1000 of the Mie scattering signals. Our current experiments were limited in nighttime. When the DPSS laser-based lidar is fixed in a sunshade area, it will act with enough accuracy. At indoor, the artificial light was no effect for Raman signal detecting by excluding for its direct insertion to the detector even if in the case of the LED-based lidar.

The hydrogen has a potential to become major energy resource. It will be popular in daily life near future. On contrary, its dangerousness is important to recognize once more. Remote sensing device for leaked hydrogen gas is essential. Compact and mini-Raman lidars will be one of the solutions.

Acknowledgements

This study was granted by Chubu Electric Power Co., Inc. from 2013 to 2016. Shikoku research institution Inc. was cooperated on the outdoor experiment, too. The author really appreciates to these companies.

Author details

Tatsuo Shiina

Address all correspondence to: shiina@faculty.chiba-u.jp

Graduate School of Engineering, Chiba University, Yayoi-cho, Inage-ku, Chiba-shi, Japan

References

[1] Gu H, Wang Z, Hu Y. Hydrogen gas sensors based on semiconductor oxide nanostructures. Sensors. 2012;**12**:5517-5550

[2] Zeng XQ, Latimer ML, Xiao ZL, Panuganti S, Welp U, Kwok WK, Xu T. Hydrogen gas sensing with networks of ultrasmall palladium nanowires formed on filtration membranes. Nano Letters. 2011;**11**:262-268

[3] Measures RM. Laser Remote Sensing: Fundamentals and Applications. New York: John Wiley & Sons; 1984

[4] Fujii T, Fukuchi T, editors. Laser Remote Sensing. Taylor & Francis; 2005

[5] Weitkamp C, editor. Lidar: Range-Resolved Optical Remote Sensing of the Atmosphere. Springer; 2005

[6] Ninomiya H, Yaeshima S, Ichikawa K, Fukuchi T. Raman lidar system for hydrogen gas detection. Optical Engineering. 2007;**46**:094301

[7] Ninomiya H, Asahi I, Sugimoto S, Shimamoto Y. Development of remote sensing technology for hydrogen gas concentration measurement using Raman scattering effect. IEEJ Transactions on Electronics, Information and Systems. 2009;**129**:1181-1185

[8] Thomas CE. Fuel cell and battery electric vehicles compared. Hydrogen Energy. 2009; **34**:6005-6020

[9] Asahi, Sugimoto S, Ninomiya H, Fukuchi T, Shiina T. Remote sensing of hydrogen gas concentration distribution by Raman lidar. Proceedings of SPIE. 2012;**8526**:85260X

[10] Shiina T. Optical design for near range lidar. Proceedings of SPIE. 2010;**7860**:78600B

[11] Suppes G. Plug-in hybrid with fuel cell battery charger. Hydrogen Energy. 2005;**30**:113-121

[12] Basquin S, Smith K, editors. Hydrogen Gas Safety Self-Study. Los Alamos National Laboratory. 2000

[13] Backx C, Wight GR, Van der Wiel MJ. Oscillator strengths (10-70eV) for absorption, ionization and dissociation in H_2, HD and D_2, obtained by an electron-ion coincidence method. Journal of Physics B: Atomic and Molecular Physics. 1976;**9**:315-333

[14] Leonard DA. Observation of Raman scattering from the atmosphere using a pulsed nitrogen ultraviolet laser. Nature. 1967;**216**:142-143

[15] Melfi SH. Remote measurement of the atmosphere using Raman scattering. Applied Optics. 1972;**11**:1605-1610

[16] Shiina T, Minami E, Ito M, Okamura Y. Optical circulator for in-line type compact lidar. Applied Optics. 2002;**41**:3900-3905

[17] Shiina T, Yoshida K, Ito M, Okamura Y. In-line type micro pulse lidar with annular beam—Experiment. Applied Optics. 2005;**44**:7407-7413

[18] Shiina T, Yoshida K, Ito M, Okamura Y. In-line type micro pulse lidar with annular beam—Theoretical approach. Applied Optics. 2005;**44**:7467-7473

[19] Grishin M, editor. Advances in Solid-State Lasers: Development and Applications, Chapter 8. INTECH; 2010

[20] Shiina T, Oguchi K, Fukuchi T. Polarization-independent optical circulator for high accuracy Faraday depolarization lidar. Applied Optics. 2012;**51**:898-904

[21] Fukuchi T, Shiina T, editors. Industrial Applications of Laser Remote Sensing. Bentham Science Publishers Ltd; 2012